Electrospun Functional Poly(ether amide) Composite Nanofibres

Xingmao Jiang[*], Shuai Liang[*], Fei Wang[*], Wangchang Geng[**]
[*] Changzhou University, School of Petrochemical Engineering, 213164, PR China
[**] Northwestern Polytechnical University, School of Science, Xi'an 710072, P.R. China
Corresponding author: E-mail: jxm@cczu.edu.cn; Fax: +86 519 86330251; Tel: +86 519 86330253

ABSTRACT

Due to its unique physical and chemical properties, poly (ether amide) (Pebax) has been widely applied in membrane separation, chemical sensing, and medical applications. Pebax composite nanofibres offer advantages such as high contact area and fast transport for ions and water molecules. (Pebax) nanofibers containing Ag nanoparticles were prepared by an electrospinning method. The Ag/Pebax nanofibers with ultra-low Ag loadings demonstrated superior antimicrobial properties against Escherichia coli and Staphylococcus aureus. Moreover, LiCl has been uniformly distributed in polyether domains of Pebax, and Pebax 2533 composite nanofibers with different amount of $LiCl{\cdot}H_2O$ were successfully fabricated by electrospinning. The electrospun nanofibres possessed high humidity sensitivity and displayed quick response and recovery.

Keywords: Pebax, Composite nanofibers, Electrospinning, antimicrobial properties, humidity sensitivity

Pebax 2533 is a kind of poly (ether amide) (Pebax) copolymer, and its structure unit consists of dodecyl amide and ether components, which offers a perfect combination of mechanical strength, breathability, flexibility, chemical resistance, no skinallergic and ease of processing. Therefore, it can be applied in many fields, such as medical materials, sports market, daily life, etc [1–3]. As medical material, it can be used to make urinary catheter, arterial catheter, PTCA (percutaneous transluminal coronary angioplasty) catheter device, infusion bags, and so forth [4–6]. If the antibacterial ability can be rendered to the Pebax by embedding Ag nanoparticles, the performance of Pebax will be dramatically improved with certainty. However, to the best of our knowledge, the preparation of Ag/Pebax composite has not been reported so far.

On the other hand, conducting polymers can be used as humidity sensor materials. However, current commonly used conducting polymers are still not sufficiently sensitive to changes in humidity, especiallyat high relative humidity and their stability and antijamming capability is poor [7]. Thus, how to overcome these shortcomings is a great challenge for humidity sensor research. Now, it has been proposed that the Pebax 2533 will form hydrophobic/hydrophilic phase-separated mesostructure under solvothermal conditions due to its composition of a hydrophobic polyamide (PA) hard domain and a soft hydrophilic polyether (PE) domain, in which PE was periodically distributed within the hydrophobic rigid PA domains [8]. It is expected that water soluble $LiCl{\cdot}H_2O$ will be located in the hydrophilic domains. However, to the best of our knowledge, Pebax-based humidity sensingmaterial has not been reported so far.

Herein, we present excellent antimicrobial material, Ag/Pebax 2533 composites and a highly efficient humidity sensing material, LiCl-doped Pebax 2533 composite nanofibers through a novel electrospinning technique, respectively. Ag/Pebax presented excellent antimicrobial properties at an ultralow $AgNO_3$ content in the precursor (0.15‰), which was much lower than that of conventional antimicrobial Ag/polymer composites reported in the literature [9-13], making Ag/Pebax composite a promising antimicrobial material with low-cost and excellent antimicrobial properties, which could be widely used in many fields in the near future. And sensors with high sensitivity among the whole relative humidity (RH) range have been obtained by appropriate loading of $LiCl{\cdot}H_2O$. Humidity sensing mechanism was analyzed by complex impedance spectra and the corresponding equivalent circuit.

We fabricated Pebax composites nanofibers with different amounts of $AgNO_3$ or $LiCl{\cdot}H_2O$ by an electrospinning method. The process started with an anhydrous Pebax solution in isopropanol and the mixture was magnetically stirred for 5 h at 60 °C to obtain a Pebax solution with a concentration of 66.7 mg mL^{-1}. Then a given amount of $AgNO_3$ or $LiCl{\cdot}H_2O$ solution was added into the Pebax solution and the content of them in Pebax composites nanofibers were controlled from 0.05 ‰ to 0.25 ‰ and 16.7 to 44.4 wt%, respectively. After sonication, the homogeneous solution was fed into a positively charged spinneret with a diameter of 0.6 mm attached to an electrospinning apparatus [14]. Finally, the Ag/Pebax composite nanofibers and LiCl-doped Pebax composite nanofibers can be obtained by the electrospinning device in the specified conditions. The composite nanofibers were collected on a filter paper or TEM grids.

The SEM and TEM images (Figure 1) indicated that the electrospun Pebax was mesh-like on a micro level formed by the connection between Pebax composite nanofibers. Especially, the interlaced $LiCl{\cdot}H_2O$–Pebax 2533 electrospun nanofibers were deposited on the pure interdigital gold electrodes as shown in Figure 1c. And the nanofibers with the diameter of about 200 nm were obviously observed in both SEM and TEM images. These

results prove that the electrospinning technique can be applied successfully to Pebax.

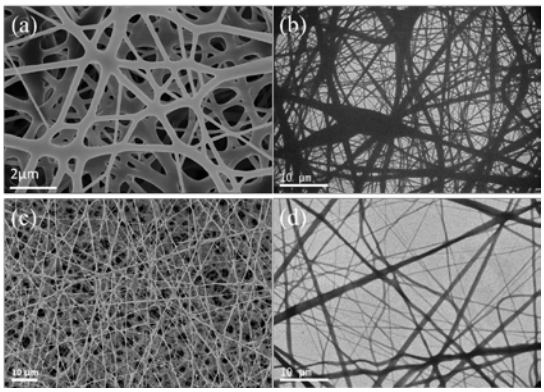

Figure 1: the SEM and TEM images of Ag/Pebax composite nanofibers (a,b) and LiCl-doped Pebax composite nanofibers(c,d).

The potential use of Ag/Pebax composite as antibacterial material was assessed by observing their antibacterial activity against two kinds of common bacteria, E. coli and S. aureus. The electrospun Pebax without Ag was evaluated in a control experiment. The bacteria were incubated in a growth medium containing various nanofibers and the antibacterial properties of samples were tested by the membrane adhering method, following the antibacterial testing standard (JISZ 2801:2010). The changes in the content of Ag had a significant effect on the antibacterial properties of Ag/Pebax composite. The number density of bacterial colony for pure Pebax was high (Figure 2a), and both of the antibacterial rate (1) and antimicrobial activity (2) were nearly zero (Figure 3); that is, there was no antibacterial activity observed for Ag free pure Pebax.

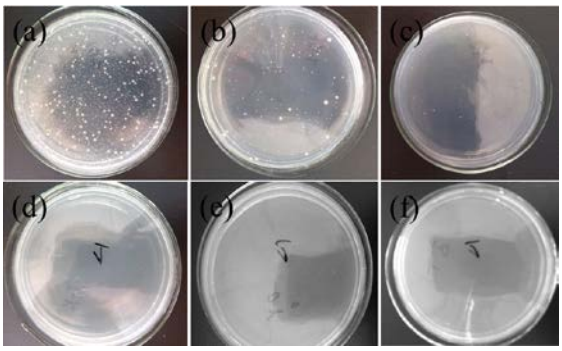

Figure 2: Comparison of the antibacterial ability of (a) Pebax, (b) Ag/Pebax-1, (c) Ag/Pebax-2, (d) Ag/Pebax-3, (e) Ag/Pebax-4, and (f) Ag/Pebax-5 against E. coli (the mass ratio of $AgNO_3$ to Pebax at 0.05 ‰, 0.10 ‰, 0.15 ‰, 0.20 ‰, and 0.25 ‰, respectively).

In contrast, the samples added with small amount of $AgNO_3$ in the Pebax precursor solution showed an inhibitory effect on E. coli and S. aureus. Although the content of $AgNO_3$ was only 0.05 ‰ (Figures 2b and 3b), the antibacterial rate against E. coli and S. aureus can reach 88.2 % and 76.1 %, respectively.

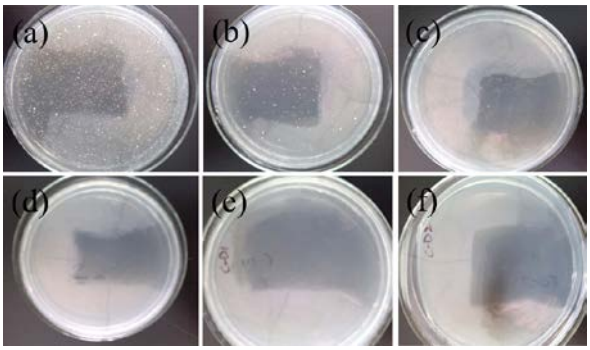

Figure 3: Comparison of the antibacterial ability of (a) Pebax, (b) Ag/Pebax-1, (c) Ag/Pebax-2, (d) Ag/Pebax-3, (e) Ag/Pebax-4, and (f) Ag/Pebax-5 against S. aureus (the mass ratio of $AgNO_3$ to Pebax at 0.05 ‰, 0.10 ‰, 0.15 ‰, 0.20 ‰, and 0.25 ‰, respectively).

Furthermore, the antibacterial properties of Ag/Pebax composite were enhanced gradually with the increase of $AgNO_3$ concentration (Figures 2b–2d, 3b–3d and 4). When the $AgNO_3$ content reached 0.15 ‰, no bacterial colony can be observed (Figures 2d and 3d) and the inhibition rates all larger than 99.9 %, and the value of antimicrobial activity against E. coli and S. aureus was 5.8 and 5.6, respectively (Figure 4). Further increasing the content of Ag failed to enhance the antibacterial properties of Ag/Pebax any more (Figures 2e–2f, 3e–3f and 4). Because the Pebax did not show antibacterial ability, Ag nanoparticles were responsible for the antibacterial ability of Ag/Pebax composites. It was reported that the antimicrobial property of material containing silver is mainly determined by the total release rate of silver ions [15]. In this work, owing to the stable particle size, the increase of Ag content will lead to the enlargement of the number and the total surface area of Ag nanoparticles; thus the release rate of silver ions was accelerated, giving rise to the improvement of antibacterial ability of Ag/Pebax composites (Figure 4). According to the antimicrobial testing standard JISZ 2801:2010, the sample whose antimicrobial activity is greater than 2 ($R > 2$) passes the antibacterial test of the strain ($R > 2$ means the antibacterial efficiency can reach 99 % or more). According to the experimental results, it can be concluded that the Ag/Pebax composite with $AgNO_3$ content larger than 0.15 ‰ presented excellent antibacterial properties, and this Ag content was much lower than that of Ag/polymer composites reported in the literature (usually larger than 1 wt.%) [9,11,12,16-19], making Ag/Pebax a promising antibacterial material with potential application in a number of fields, such as biomedical materials, sports apparatus, and laminating films.

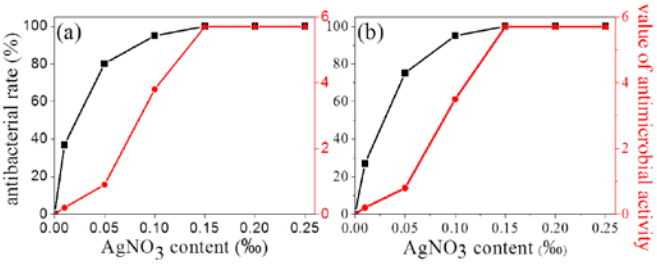

Figure 4: The antibacterial rate and antimicrobial activity of Ag/Pebax against (a) E. coli and (b) S. aureus as a function of $AgNO_3$ content in the precursor.

Figure 5a reveals the hysteresis data of $LiCl{\cdot}H_2O$–Pebax 2533 composite with $LiCl{\cdot}H_2O$ content at 44.4 wt%. As we can see from Figure 5a this as-synthesized sample has a negligible hysteresis, indicating that this material is a kind of promising humidity sensing material. Response and recovery time are also very important to a humidity sensor. Figure 5b provides the response and recovery time curve of $LiCl{\cdot}H_2O$–Pebax 2533 composite with $LiCl{\cdot}H_2O$ content at 44.4 wt%. According to the literature report [20], the time taken by a sensor to achieve 90 % of the total impedance change is defined as the response time or recovery time. For the sample of $LiCl{\cdot}H_2O$–Pebax 2533 composite with $LiCl{\cdot}H_2O$ content at 44.4 wt%, the response time was about 30 s with relative humidity increasing from 11% RH to 95% RH, and the recovery time was 80 s with relative humidity decreasing from 95% RH to 11% RH.

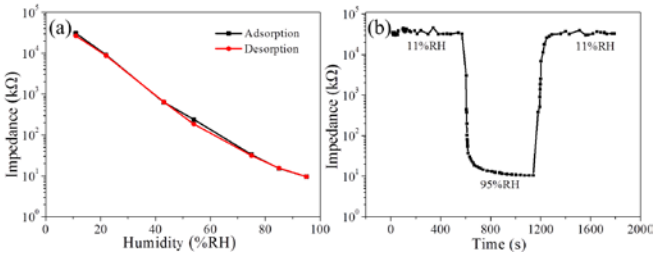

Figure 5: (a) Hysteresis, (b) Response and recovery curve of $LiCl{\cdot}H_2O$-Pebax 2533 composite with $LiCl{\cdot}H_2O$ content at 44.4 wt% (measuring frequency: 100 Hz, voltage: 1 V).

In order to explain the humidity sensing mechanism of this $LiCl{\cdot}H_2O$–Pebax 2533 composite material, complex impedance plots and the corresponding equivalent circuits (inset) of $LiCl{\cdot}H_2O$–Pebax 2533 composite with $LiCl{\cdot}H_2O$ content at 44.4 wt% under different relative humidities were provided as shown in Figure 6. The measuring frequency was from 50 Hz to 100 kHz, the horizontal and vertical axis value corresponding to the real and imaginary part of the complex impedance of the sensing material, respectively. When the relative humidity was low (22% RH), few water molecules were adsorbed on the surface of sensing material, and proton migrates only by hopping from site to site across the sample surface [21], so the resistance of the sensor under this relative humidity mainly comes from the intrinsic high resistance of Pebax 2533, and its impedance is mainly determined by the capacitance of sensing film. The corresponding complex impedance plot looks like a straight line and the equivalent circuit can be modeled by a constant phase element (CPE) [22] as shown in inset of Figure 6a, the film capacitance calculated from the constant phase element was 1.6×10^{-11} F. When RH increased to the middle region (43% and 54% RH), more water molecules are adsorbed and serial water layer is formed. According to the ion transfer mechanism of Grotthuss [23], the serial water layer accelerates the transfer of H^+ and H_3^+O dissociated from the adsorbed water layer. Therefore, the resistance of the sensing film decreased, the film resistance decreased from $2.87 \times 10^7\,\Omega$ to $7.39 \times 10^6\,\Omega$. In addition, the film capacitance value increased gradually because that the adsorbed water increased the dielectric constant of the sensing film. The corresponding complex impedance plot is a semicircle as shown in Figure 6b and c and the equivalent circuit can bemodeled by the parallel combination of a resistor (R) and a capacitor (C) as shown in inset of Figure 6b and c. When RH further increased to 75% RH, more water molecules are adsorbed and serial water layer can reach three layers according to literature [24]. According to the model of ion transport mechanism reported by Casalbore Miceli [25], Li^+ dissociated from the dissolved LiCl become free ions after getting rid of the interaction of the opposite charges Cl^- and the resistance of the sensing film decreased sharply due to the quick transfer of the free ions. In addition, under this RH, water molecules also accumulated at the interface between sensing filmand electrode. Hence, the interface resistance and capacitance also contributed to the impedance of the sensor under this RH. We can see that the complex impedance plot includes a semicircle in left side (high frequency region) and a short line in right side (low frequency region) as shown in Figure 6d. The semicircle is caused by the resistance R_f and capacitance C_f of $LiCl{\cdot}H_2O$–Pebax 2533 film. And the short line in low frequency side is caused by the diffusion process of ions or charge carriers (mainly includes H^+ and free Li^+) at the sensing film/electrode interface [22]. Under this RH, equivalent circuit shown in inset of Figure 6d can account for the sensing mechanism. When the relative humidity increased to higher RH region (85% RH, 95% RH), due to the hygroscopicity of LiCl, water multilayers formed both in sensing film and in sensing film/electrode interface. More and more LiCl dissolved in these water layers to form a solution, the dissolved Li^+ and Cl^- have a big contribution to the conduction of the sensing film, so the sensing film resistanceand interface resistance further decreased. Under this RH range (85–95% RH), the LiCl solution resistance also contributed to the conduction of the sensor and it decreased with the increasing RH. Therefore, we can use the equivalent circuit shown in inset of Figure 6e and f to describe sensing mechanism under this RH range. Interestingly, the film capacitance C_f increased nearly two orders of magnitude (from 3.7×10^{-10} F to 3.5×10^{-8} F) when RH increased from 85% RH to 95% RH. Our opinion is that under 95% RH, the internal of the sensing

material are fully filled by adsorbed water which will greatly increase the dielectric constant of the sensing material, so the capacitance also increased sharply.

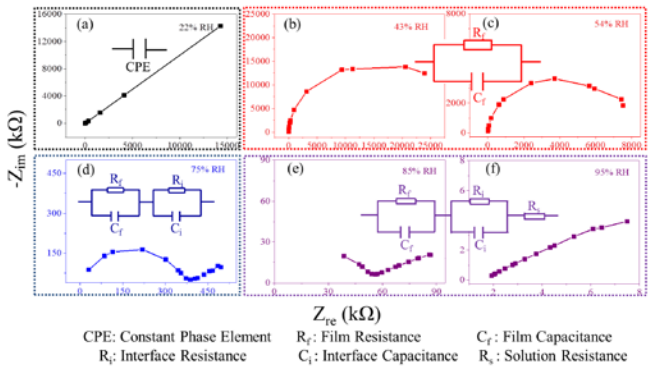

Figure 6: Complex impedance plots and the corresponding equivalent circuits (inset) of LiCl·H_2O-Pebax 2533 composite with LiCl·H_2O content at 44.4 wt% under different relative humidities (measuring frequency: 16 frequency points from 50 Hz to 100 kHz, voltage: 1 V).

In summary, this study has described a simple route to prepare Ag/Pebax composite nanofibers and LiCl-doped Pebax composite nanofibers via an electrospinning process. Ag nanoparticles with an average diameter of ca.15 nm were dispersed homogeneously in Pebax nanofibers. The antimicrobial activities against E. coli and S. aureus were evaluated by membrane adhering method. Study results indicated that the Ag/Pebax composites presented outstanding antimicrobial properties at ultralow Ag content; for example, the inhibition rate can reach >99.9% and antimicrobial activity against E. coli and S. aureus was 5.8 and 5.6 at the critical value of $AgNO_3$ content (0.15 ‰), respectively, which suggested that the Ag/Pebax composite can be used as a promising antimicrobial material. And study results of humidity sensing performance indicated that LiCl·H_2O–Pebax 2533 composite with LiCl·H2O content at 44.4 wt% exhibited the best sensing property. Free Li ion dissociated from dissolved LiCl at higher relative humidity region play an important role in improving the sensing propertyof this material. The present work proved that electrospinning technology is a convenience and effective way to prepare LiCl/block polymer composite-based humidity sensing materials with high sensitivity.

This work was financially supported by the National Natural Science Foundation of China under Grant (no. 21373034); Jiangsu Key Laboratory of Advanced Catalytic Material and Technology; and Key Laboratory of Fine Petrochemical Engineering and PAPD of Jiangsu Higher Education Institutions.

REFERENCES

[1] C. L. Restuccia and C. LoFaro, U.S. Patent. No. 0170746 A1. 2010.
[2] N.L. Le, Y. Wang, T.S. Chung, J. Membr. Sci. 379,174–183, 2011.
[3] C. Cheng, R. Tang, F. Xi, Rapid Commun. 26,744–749, 2005.
[4] T. H. Gilman, U.S. Patent. no. 0015192 A1, 2012.
[5] D. J. Buckley, D. G.Wildes,W. Lee, andW. B. Griffin, U.S. Patent 0256502 A1, 2010.
[6] N. L. Le, Y.Wang, and T. S. Chung, J Membrane Sci. 379(1-2) 174–183, 2011.
[7] K. Jiang, T. Fei, T. Zhang, Sens. Actuators B. 199, 1–6, 2014.
[8] X.M. Jiang, C.J. Brinker, Chem. Commun. 466, 123–6125, 2010.
[9] M. S. Islam and J. H. Yeum, Colloid Surf. A-Physicochem. Eng. Asp. 436, 279–286, 2013.
[10] H. H. Chae, B. Kim, K. S. Yang, and J. I. Rhee, Synthetic Met. 161, 2124–2128, 2011.
[11] C. D. Saquing, J. L. Manasco, and S. A. Khan, Small, 5, 944–951, 2009.
[12] F. A. Sheikh, N. A. M. Barakat, M. A. Kanjwal et al., Macromol. RES. 17, 688–696, 2009.
[13] K. A. Khalil, H. Fouad, T. Elsarnagawy, and F. N. Almajhdi, Int. J. Electrochem. Sci. 8, 3483–3493, 2013.
[14] Q. Shi, N. Vitchuli, J. Nowak et al., Eur. Polym. J. 47, 1402–1409, 2011.
[15] S. Zhang, F. Peng, H. Wang, H. Yu, J. Yang, and H. Zhao, Catal. Commun. 12, 689–693, 2011.
[16] Y. Matsumura, K. Yoshikata, S. Kunisaki, and T. Tsuchido, Appl. Environ. Microb. 69, 4278–4281, 2003.
[17] D. P. Dowling, K. Donnelly, M. L. McConnell, R. Eloy, and M. N. Arnaud, Thin Solid Films, 398-399, 602–606, 2001.
[18] Q. Shi, N. Vitchuli, J. Nowak et al., Journal of Materials Chemistry, 21, 10330–10335, 2011.
[19] A. Celebioglu, Z. Aytac, O. C. Umu, A. Dana, T. Tekinay, and T. Uyar, Carbohydrate Polymers, 99, 808–816, 2014.
[20] S. Agarwal, G.L. Sharma, Sens. Actuators B. 85, 205–211, 2002.
[21] J.H. Anderson, G.A. Parks, J. Phys. Chem. 72, 3662–3668, 1968.
[22] W.C. Geng, Q. Yuan, X.M. Jiang, J.C. Tu, L.B. Duan, J.W. Gu, Q.Y. Zhang , Sens. Actuators B. 174, 513–520, 2012.
[23] F.M. Ernsberger, J. Am. Ceram. Soc. 11, 747–750, 1983.
[24] C.L. Li, Y.T. Ma, Y. Li, F.H. Wang, Corros. Surf. 52, 3677–368, 2010.
[25] G. Casalbore-Miceli, M.J. Yang, N. Camaioni, C.M. Mari, Y. Li, H. Sun, M. Ling, Solid State Ionics 131, 311–321, 2000.